Journal of Prevention, Diagnosis and Management of Human Diseases
Vol: 06, No. 02, July-Dec 2026
ISSN: 2799-1202, DOI: 10.55529/jpdmhd.62.54.62

Research Paper

Interpretable lung-field texture analysis of chest radiographs for tuberculosis triage: Segmentation, zonal patterns and the WHO target product profile

Sadyrova Nurgul[1*], Muratov Zhanibek[2], Tashpolotova Anarkan[3]

[1*]Department of Clinical Disciplines, Jalal-Abad International University, 720906, 24 Kurmanbek Str., Manas, Kyrgyzstan.

[2]Department of Clinical Disciplines, Jalal-Abad International University, Osh State University, Osh International Medical University, 720906, 24 Kurmanbek Str., Manas, Kyrgyzstan.

[3]Department of Clinical Disciplines, Jalal-Abad International University, 720906, 24 Kurmanbek Str., Manas, Kyrgyzstan.

Article Info

Article History:
Received: 11 April 2026
Revised: 23 June 2026
Accepted: 01 July 2026
Published: 17 August 2026

Keywords:
Tuberculosis
Chest Radiography
Computer-Aided Detection
Lung Segmentation
Texture Analysis
Target Product Profile

ABSTRACT

Background: Computer-aided detection (CAD) of tuberculosis (TB) on chest radiographs is recommended by the World Health Organization (WHO) for screening and triage, and a triage test should reach at least 90% sensitivity and 70% specificity.

Objective: To evaluate a transparent, segmentation-based approach to TB detection and to compare its performance with the WHO triage target.

Methods: The NLM Montgomery County chest X-ray set was used (138 posteroanterior radiographs from 134 patients; 58 with TB, 80 normal), with expert lung masks and radiology readings. A compact U-Net was trained to segment lung fields using patient-grouped five-fold cross-validation. A total of 110 intensity, texture (grey-level co-occurrence and local binary pattern) and left–right asymmetry features were computed for the upper, middle and lower zone of each lung. Logistic regression and random forests were evaluated with 20 repetitions of patient-grouped cross-validation.

Results: The U-Net segmented lungs with a mean Dice coefficient of 0.970, but agreement was lower for TB than normal radiographs (0.960 vs 0.978, $p = 4 \times 10^{-6}$); the four worst segmentations all excluded opaque, diseased lung such as pleural effusion. Lung-field features classified TB with an area under the receiver operating characteristic curve (AUROC) of 0.882 (manual masks) and 0.895 (U-Net masks), versus 0.815 for fixed image regions without lung masks. Upper-zone features alone reached an AUROC of 0.849, versus 0.592 for middle and 0.653 for lower zones. At 70% specificity, sensitivity was 86.2% (95% CI 76.4–94.6%) with manual masks and 91.4% (80.0–98.4%) with U-Net masks. Sensitivity was lower for inactive or healed disease (78.9%) than active disease (89.5%). False positives were concentrated in older healthy individuals (42% vs 13% under 40 years).

Conclusions: Interpretable lung-field analysis approaches but does not reliably meet the WHO triage target on this dataset, with the target met at best marginally and with wide uncertainty. Larger, prospective validation attending to disease activity and age is required.

Corresponding Author:
Sadyrova Nurgul
Department of Clinical Disciplines, Jalal-Abad International University, 720906, 24 Kurmanbek Str., Manas, Kyrgyzstan
Email: sadyrova.n73@mail.ru

Copyright © 2026 The Author(s). This is an open access article distributed under the Creative Commons Attribution License, (http://creativecommons.org/licenses/by/4.0/) which permits unrestricted use, distribution, and reproduction in any medium, provided the original work is properly cited.

1. INTRODUCTION

Tuberculosis remains the leading cause of death from a single infectious agent; an estimated 10.7 million people fell ill with TB and 1.23 million died from it in 2024 [1]. Many cases are never diagnosed or notified, and early detection through systematic screening and triage is central to TB prevention and control. Chest radiography is highly sensitive for pulmonary TB, but its interpretation requires trained readers who are scarce in high-burden settings. Since 2021, WHO has recommended computer-aided detection (CAD) software as an alternative to human readers for screening and triage in individuals aged 15 years and older [2]. For a triage test, WHO's target product profile (TPP) specifies a minimum sensitivity of 90% and specificity of 70% [3].

Deep learning CAD products now achieve high accuracy in large evaluations [4], [5], [6], but they are typically proprietary, require large training sets and give little insight into the image features that drive their decisions. Shortcut learning, in which models rely on burned-in labels, devices or patient positioning rather than on lung pathology, is a well-documented risk for chest radiograph classifiers [7], [8]. Interpretable approaches that restrict analysis to segmented lung fields and use explicit intensity and texture features [9] are less prone to such shortcuts, can be developed on small local datasets and make it possible to check whether the model attends to the lung regions where TB is expected.

This study evaluates such an approach on a public dataset of real radiographs with expert lung masks and radiology readings [10]. It asks four questions: how accurately a compact U-Net segments the lung fields, particularly in diseased lungs; how well zone-wise lung-field features distinguish TB from normal radiographs; which lung zones carry the most information; and whether performance meets the WHO triage target, overall and in clinically relevant subgroups.

2. METHODOLOGY

2.1 Data

The Montgomery County chest X-ray set was collected by the TB control programme of the Department of Health and Human Services of Montgomery County, Maryland, USA, and released by the U.S. National Library of Medicine [10]. It contains 138 posteroanterior radiographs (4,020 × 4,892 or 4,892 × 4,020 pixels; 12-bit, provided as PNG), of which 80 are normal and 58 show manifestations of TB, together with manual segmentation masks of both lungs [11] and a text file with the patient's sex, age and the radiologist's reading. The data were obtained from a public repository that includes the complete set [12]. Three patients had more than one radiograph (two with two and one with three images, identified from

cross-references in the readings and identical reports), giving 134 patients. Across the 138 radiographs, patients were aged 4–89 years (median 40); 74 radiographs were from female and 63 from male patients, and one had no recorded sex. Because three patients contributed more than one radiograph, these counts are at the image level. Patients with TB were older than those with normal radiographs (median 47 vs. 33.5 years). The readings of TB cases were coded as active or other findings (n = 38), inactive or healed disease, such as calcified granulomas or stable scars (n = 19), or no report (n = 1); 13 mentioned pleural involvement and 37 mentioned the upper lobes or apex. Figure 1 shows real radiographs with the expert masks and readings. The images are anonymised and publicly released.

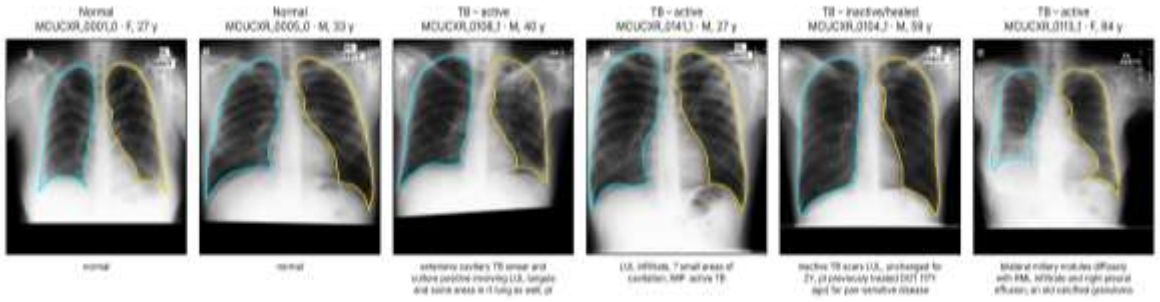


Figure 1. Real Posteroanterior Radiographs from the Montgomery County Set with the Expert Lung Masks (Cyan: Patient's Right Lung; Yellow: Patient's Left Lung), Patient Sex and Age, and the Beginning of the Radiologist's Reading

2.2 Lung Segmentation

Images were resized to 512 × 512 pixels. A compact U-Net [13] (five resolution levels with 8–96 channels) was trained on 256 × 256-pixel images with a combined binary cross-entropy and Dice loss, the Adam optimiser and light intensity augmentation for 40 epochs. Five-fold cross-validation, stratified by diagnosis and grouped by patient, was used so that every radiograph was segmented by a model that had not seen that patient. Predicted masks were upsampled to 512 × 512 pixels, the two largest connected components were kept and assigned to the right or left lung by position, and agreement with the expert masks was measured by the Dice coefficient.

2.3 Zone-Wise Lung-Field Features

Each radiograph was enhanced with contrast-limited adaptive histogram equalisation [14]. Each lung was divided into upper, middle and lower thirds of its vertical extent, and for each of the six zones 12 features were computed: mean, standard deviation, skewness, kurtosis and 10th and 90th percentiles of intensity; grey-level co-occurrence contrast, homogeneity, energy and correlation (32 grey levels, distances 2 and 4 pixels, two directions) [15]; and the entropy and non-uniform fraction of uniform local binary patterns [16]. The absolute left–right difference of each zone feature (36 asymmetry features), the lung area as a fraction of the image and the right-to-left area ratio were added, giving 110 features. Features were computed with expert masks, with U-Net masks and, as a control without lung segmentation, with two fixed rectangular boxes covering the left and right halves of the chest. Image processing used scikit-image [17] and PyTorch [18].

2.4 Classification and Evaluation

L2-regularised logistic regression (standardised features, C = 0.05) and random forests [19] (500 trees) were evaluated with five-fold cross-validation, stratified by diagnosis and grouped by patient [20], repeated 20 times with different splits [21]. The AUROC was computed for each repetition, and the out-of-fold scores averaged over repetitions were used for ROC analysis. In line with the WHO TPP [3], sensitivity at a specificity of at least 70% and specificity at a sensitivity of at least 90% were reported, with 95% confidence intervals from 2,000 bootstrap samples of patients. To identify where the information lies, logistic regression was also trained on subsets of features: each zone level, the asymmetry features,

intensity or texture features only and lung shape only. At the operating point with at least 70% specificity, sensitivity was compared between subgroups of TB cases defined from the readings, and the false-positive rate between age groups and sexes. Reporting follows the relevant items of STARD 2015 [22].

3. RESULTS AND DISCCUSSION

3.1 Lung Segmentation

The U-Net segmented the lung fields with a mean Dice coefficient of 0.970 (median 0.977, fold means 0.967–0.978). Agreement was significantly lower for radiographs with TB than for normal radiographs (mean 0.960 vs. 0.978; Mann–Whitney p = 4 × 10−6). Four radiographs had a Dice coefficient below 0.90, all from TB patients. In each of them, the network excluded opaque lung that the expert had included within the lung boundary: a large right pleural effusion, a right pleural peel with atelectasis, a right effusion with upper-lobe infiltrate and active TB with heart failure (Figure 2). Segmentation errors were therefore concentrated in exactly the regions that carry the pathology.

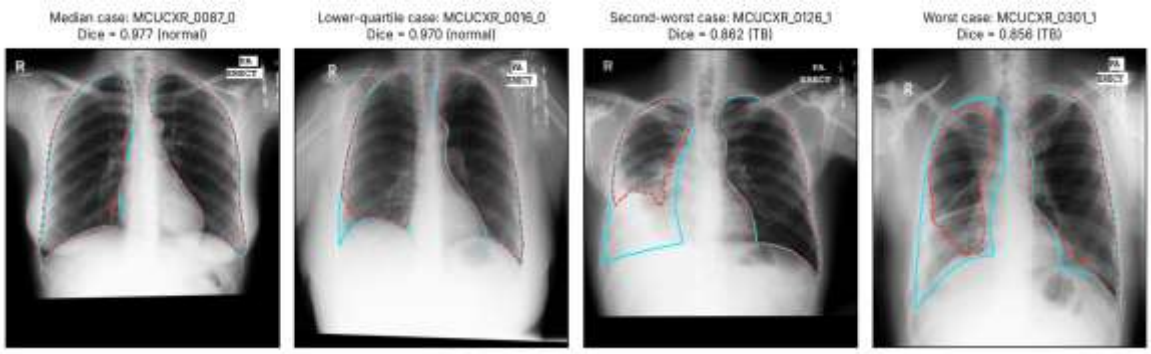


Figure 2. Automatic U-Net Lung Segmentation (Red, Dashed) Compared with the Expert Masks (Cyan) for the Median, Lower-Quartile and Two Worst Cases (Patient-Grouped Cross-Validation). In Both Worst Cases, a Right Pleural Effusion or Pleural Peel is Excluded from the Automatic Mask.

3.2 TB Classification

Table *1* and Figure 3 (left) summarise the classification results. With features from the expert lung masks, logistic regression reached a mean AUROC of 0.882 ± 0.010 over 20 repetitions, and with features from the U-Net masks 0.895 ± 0.009; these ranges are standard deviations over the 20 repetitions, not confidence intervals, and they overlapped widely. Without lung segmentation, features from fixed image regions gave a clearly lower AUROC of 0.815 ± 0.016. Logistic regression performed better than random forests in all settings. At the operating point with at least 70% specificity, the sensitivity of logistic regression was 86.2% (95% CI 76.4–94.6%) with expert masks and 91.4% (80.0–98.4%) with U-Net masks, and at 90% sensitivity the specificity was 53.8% and 70.0%. The model using U-Net masks therefore touched the WHO minimum triage target at its point estimate, but the lower confidence limits of both sensitivity and specificity lay well below the target, and the model using expert masks did not reach it.

Table 1. TB Classification Performance with Patient-Grouped Cross-Validation (20 Repetitions). AUROC is Mean ± SD over Repetitions; Operating Points and 95% Confidence Intervals (Patient Bootstrap) Are from Scores Averaged over Repetitions. The WHO Minimum Triage Target is Sensitivity ≥ 90% with Specificity ≥ 70%.

Features	Classifier	AUROC (Mean ± SD)	AUROC, Pooled (95% CI)	Sensitivity at Sp ≥ 70% (%)	Specificity at Se ≥ 90% (%)
Lung fields, expert masks	Logistic regression	0.882 ± 0.010	0.888 (0.826–0.941)	86.2 (76.4–94.6)	53.8 (40.7–84.7)

	Random forest	0.860 ± 0.009	0.866 (0.798–0.927)	86.2 (76.8–94.5)	45.0 (18.2–83.9)
Lung fields, U-Net masks	Logistic regression	0.895 ± 0.009	0.903 (0.848–0.949)	91.4 (80.0–98.4)	70.0 (55.7–87.5)
	Random forest	0.857 ± 0.008	0.865 (0.801–0.924)	87.9 (76.6–95.7)	47.5 (25.6–82.9)
Fixed regions, no lung mask	Logistic regression	0.815 ± 0.016	0.821 (0.747–0.888)	79.3 (65.5–90.0)	45.0 (28.4–70.7)
	Random forest	0.802 ± 0.014	0.812 (0.731–0.887)	75.9 (65.1–89.1)	37.5 (22.1–68.6)

3.3 Where the Information Lies

Feature subsets showed a clear zonal pattern (Figure 3, right). Features from the upper zones of both lungs alone reached an AUROC of 0.849 ± 0.011, close to that of all features, whereas middle-zone (0.592) and lower-zone (0.653) features were much weaker. Left–right asymmetry features alone gave 0.805, reflecting the frequently unilateral distribution of disease. Texture features (0.855) were more informative than intensity features (0.824), and lung area and the right-to-left area ratio carried little information (0.543). The model thus relied mainly on texture in the upper lung zones, where post-primary TB typically manifests.

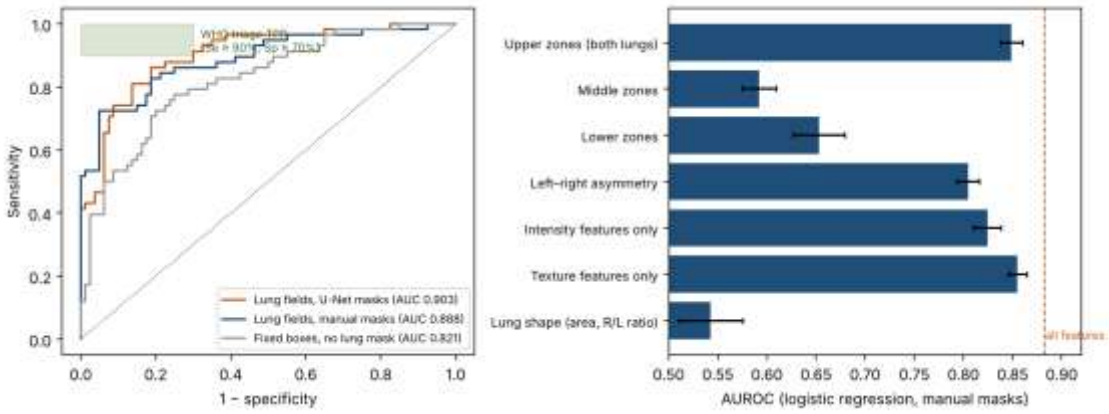


Figure 3. Left: ROC Curves of Logistic Regression with Lung-Field Features from U-Net Masks, Expert Masks and Fixed Regions Without Lung Masks (Scores Averaged over 20 Cross-Validation Repetitions); The Shaded Area Marks the WHO Minimum Triage Target. Right: AUROC of Logistic Regression Trained on Subsets of the Expert-Mask Features (Mean ± SD over 20 Repetitions); The Dashed Line Marks All Features

3.4 Subgroups

At the operating point with at least 70% specificity (expert masks, logistic regression; overall sensitivity 86.2%, specificity 75.0%), sensitivity was 89.5% for active disease or other findings (34 of 38) but 78.9% for inactive or healed disease (15 of 19) (Table 2). Sensitivity was similar with and without pleural involvement (84.6% and 86.7%) and with and without upper-lobe involvement (86.5% and 85.7%), but lower when the reading described only left-sided disease (70.6%, 12 of 17) than right-sided (94.4%) or bilateral disease (92.3%); the remaining 10 of the 58 TB readings did not specify laterality. False positives were strongly associated with age: 42.4% of normal radiographs from individuals aged 40 years or older were classified as TB, compared with 12.8% of those under 40. Sensitivity was also higher in men (94.6%) than in women (71.4%), although these groups overlapped with the age groups and were small.

Table 2. Sensitivity and False-Positive Rate by Subgroup at the Operating Point with Specificity ≥ 70% (Expert Masks, Logistic Regression).

Group	N	Classified as TB (%)
TB: active disease or other findings	38	89.5
TB: inactive or healed disease	19	78.9
TB: pleural involvement / none	13 / 45	84.6 / 86.7
TB: left only / right only / bilateral	17 / 18 / 13	70.6 / 94.4 / 92.3
TB: women / men	21 / 37	71.4 / 94.6
TB: age < 40 / ≥ 40 years	21 / 37	81.0 / 89.2
Normal: age < 40 years (false positives)	47	12.8
Normal: age ≥ 40 years (false positives)	33	42.4

3.5 Discussion

This study shows that a transparent pipeline, consisting of lung segmentation and zone-wise intensity and texture features with a linear classifier, distinguishes TB from normal chest radiographs on real data with an AUROC of about 0.88–0.90. This is similar to the performance originally reported on this dataset with a larger feature set [9] and below that of commercial deep learning products evaluated on large populations [4]. Restricting the analysis to the lung fields improved the AUROC by about 0.07 compared with fixed image regions, which supports the value of segmentation both for accuracy and for preventing models from learning from labels, markers and anatomy outside the lungs [7], [8]. The radiographs in Figure 1 carry burned-in text and markers that a whole-image model could exploit.

The zonal analysis provides a plausibility check that black-box models lack. The upper zones carried almost all of the discriminative information, in agreement with the predilection of post-primary TB for the apical and posterior segments of the upper lobes, and asymmetry features were informative because disease is often unilateral. Such explicit evidence makes it easier for clinicians and programme managers to judge whether a CAD system is detecting disease for the right reasons.

Measured against the WHO triage target [3], however, the results are sobering. Only the U-Net-mask model reached 90% sensitivity at 70% specificity, and with 58 TB cases the lower confidence limit of sensitivity was 80%. A triage test that misses one in five cases would not be acceptable, and the evidence on this dataset is insufficient to show that the target is met. Two subgroup findings are relevant for programme use. First, inactive or healed disease was detected less often than active disease. In screening, detection of old lesions is not a goal in itself, but such lesions still trigger confirmatory testing, so the case mix strongly affects the observed sensitivity. Second, false positives were concentrated in older individuals, whose radiographs more often show age-related changes. Because TB patients in this dataset were older than controls, part of the apparent discrimination may reflect age rather than TB, and in older screening populations the specificity would probably be lower than estimated here. Threshold selection for CAD should therefore consider the age structure of the target population, in line with WHO guidance that CAD thresholds should be calibrated for the population in which the software is used [2].

A further observation concerns segmentation. Although the U-Net reached a high average Dice coefficient, its largest errors occurred in diseased lungs, where it excluded opaque regions such as pleural effusions. The slightly higher AUROC with U-Net masks should therefore not be interpreted as better segmentation; excluding diseased lung changes the zone boundaries and features in ways that may happen to be discriminative here but are unlikely to generalise. Segmentation quality should be reported separately for abnormal radiographs, and pipelines should be robust to masks that miss diseased regions.

The study has limitations. The dataset is small (58 TB cases), comes from a single low-burden screening programme and was acquired with one system; the reference standard is the radiologist's reading supported by clinical information rather than bacteriological confirmation for every case, and the coding of subgroups from free-text readings is approximate. Repeated radiographs of three patients were handled by grouping, but other undetected repeats cannot be excluded. Only hand-crafted features and simple classifiers were evaluated, and no external test set was available. Subgroup estimates are based on small numbers and should be regarded as exploratory.

4. CONCLUSION

On real chest radiographs from the Montgomery County TB screening programme, an interpretable pipeline of U-Net lung segmentation and zone-wise texture features detected TB with an AUROC of 0.88–0.90, with most of the information located in the upper lung zones. Restricting analysis to the lung fields clearly improved performance over fixed image regions. Segmentation errors were concentrated in diseased lungs, and the WHO minimum triage target of 90% sensitivity at 70% specificity was reached at best marginally and with wide uncertainty. Sensitivity was lower for inactive disease, and false positives were concentrated in older individuals. Interpretable CAD can help to understand and audit TB detection, but any system intended for screening or triage must be validated prospectively in the target population, with bacteriological confirmation and with operating thresholds chosen for the local age structure and case mix.

Author Contribution Statement

Name of Author	C	M	So	Va	Fo	I	R	D	O	E	Vi	Su	P	Fu
Sadyrova Nurgul		✓	✓		✓				✓		✓			✓
Muratov Zhanibek		✓	✓	✓		✓		✓				✓		
Tashpolotova Anarkan	✓		✓		✓		✓		✓		✓		✓	✓

C: **C**onceptualization
M : **M**ethodology
So : **So**ftware
Va : **Va**lidation
Fo : **Fo**rmal analysis
I : **I**nvestigation
R : **R**esources
D : **D**ata Curation
O : Writing - **O**riginal Draft
E : Writing - Review & **E**diting
Vi : **Vi**sualization
Su : **Su**pervision
P : **P**roject administration
Fu : **Fu**nding acquisition

Acknowledgments

The authors acknowledge the Department of Health and Human Services of Montgomery County, Maryland, USA, and the U.S. National Library of Medicine for creating and releasing the Montgomery County chest X-ray set, and the maintainers of the public repository used to obtain it, and the researchers whose works have been cited in this study.

Funding Information

This research has received no external funding.

Conflict of Interest Statement

No conflict of interest.

Informed Consent

Not Applicable. The study used only publicly available, anonymised images.

Ethical Approval

Not Applicable. The study is a secondary analysis of publicly available, anonymised images and involved no human participants.

Data Availability

This study uses the publicly available NLM Montgomery County chest X-ray set [10], obtained from a public repository [12]. No new datasets were created. The analysis code is available from the corresponding author on reasonable request.

Use of Generative AI

Generative AI tools were not used to generate the scientific content, data, analyses or results of this study. Any AI-assisted language editing was reviewed and revised by the authors, who take full responsibility for the content of this article.

REFERENCES

[1] World Health Organization, Global Tuberculosis Report 2025. Geneva, Switzerland: WHO, 2025. www.who.int/teams/global-programme-on-tuberculosis-and-lung-health/tb-reports/global-tuberculosis-report-2025

[2] World Health Organization, WHO Consolidated Guidelines on Tuberculosis. Module 2: Screening – Systematic Screening for Tuberculosis Disease. Geneva, Switzerland: WHO, 2021. www.who.int/publications/i/item/9789240022676

[3] World Health Organization, High-Priority Target Product Profiles for New Tuberculosis Diagnostics: Report of a Consensus Meeting (WHO/HTM/TB/2014.18). Geneva, Switzerland: WHO, 2014. www.who.int/publications/i/item/WHO-HTM-TB-2014.18

[4] Z. Z. Qin et al., "Tuberculosis detection from chest x-rays for triaging in a high tuberculosis-burden setting: An evaluation of five artificial intelligence algorithms," The Lancet Digital Health, vol. 3, no. 9, pp. e543–e554, 2021. doi.org/10.1016/S2589-7500(21)00116-3

[5] M. Harris et al., "A systematic review of the diagnostic accuracy of artificial intelligence-based computer programs to analyze chest x-rays for pulmonary tuberculosis," PLoS ONE, vol. 14, no. 9, Art. no. e0221339, 2019. doi.org/10.1371/journal.pone.0221339

[6] P. Lakhani and B. Sundaram, "Deep learning at chest radiography: Automated classification of pulmonary tuberculosis by using convolutional neural networks," Radiology, vol. 284, no. 2, pp. 574–582, 2017. doi.org/10.1148/radiol.2017162326

[7] J. R. Zech, M. A. Badgeley, M. Liu, A. B. Costa, J. J. Titano, and E. K. Oermann, "Variable generalization performance of a deep learning model to detect pneumonia in chest radiographs: A cross-sectional study," PLoS Medicine, vol. 15, no. 11, Art. no. e1002683, 2018. doi.org/10.1371/journal.pmed.1002683

[8] A. J. DeGrave, J. D. Janizek, and S.-I. Lee, "AI for radiographic COVID-19 detection selects shortcuts over signal," Nature Machine Intelligence, vol. 3, no. 7, pp. 610–619, 2021. doi.org/10.1038/s42256-021-00338-7

[9] S. Jaeger et al., "Automatic tuberculosis screening using chest radiographs," IEEE Transactions on Medical Imaging, vol. 33, no. 2, pp. 233–245, 2014. doi.org/10.1109/TMI.2013.2284099

[10] S. Jaeger, S. Candemir, S. Antani, Y.-X. J. Wáng, P.-X. Lu, and G. Thoma, "Two public chest X-ray datasets for computer-aided screening of pulmonary diseases," Quantitative Imaging in Medicine and Surgery, vol. 4, no. 6, pp. 475–477, 2014. doi.org/10.3978/j.issn.2223-4292.2014.11.20

[11] S. Candemir et al., "Lung segmentation in chest radiographs using anatomical atlases with nonrigid registration," IEEE Transactions on Medical Imaging, vol. 33, no. 2, pp. 577–590, 2014. doi.org/10.1109/TMI.2013.2290491

[12] A. Maity et al., "CXR-Lung-Segmentation-DCNN" (repository containing the NLM Montgomery County CXR set), GitHub. Accessed: Oct. 2026. github.com/arunitmaity/CXR-Lung-Segmentation-DCNN

[13] O. Ronneberger, P. Fischer, and T. Brox, "U-Net: Convolutional networks for biomedical image segmentation," in Medical Image Computing and Computer-Assisted Intervention – MICCAI 2015, LNCS vol. 9351, Springer, 2015, pp. 234–241. doi.org/10.1007/978-3-319-24574-4_28

[14] K. Zuiderveld, "Contrast limited adaptive histogram equalization," in Graphics Gems IV, P. S. Heckbert, Ed. San Diego, CA, USA: Academic Press, 1994, pp. 474–485. doi.org/10.1016/B978-0-12-336156-1.50061-6

[15] R. M. Haralick, K. Shanmugam, and I. Dinstein, "Textural features for image classification," IEEE Transactions on Systems, Man, and Cybernetics, vol. SMC-3, no. 6, pp. 610–621, 1973. doi.org/10.1109/TSMC.1973.4309314

[16] T. Ojala, M. Pietikäinen, and T. Mäenpää, "Multiresolution gray-scale and rotation invariant texture classification with local binary patterns," IEEE Transactions on Pattern Analysis and Machine Intelligence, vol. 24, no. 7, pp. 971–987, 2002. doi.org/10.1109/TPAMI.2002.1017623

[17] S. van der Walt et al., "scikit-image: Image processing in Python," PeerJ, vol. 2, Art. no. e453, 2014. doi.org/10.7717/peerj.453

[18] A. Paszke et al., "PyTorch: An imperative style, high-performance deep learning library," in Advances in Neural Information Processing Systems (NeurIPS), vol. 32, 2019, pp. 8024–8035. doi.org/10.48550/arXiv.1912.01703

[19] L. Breiman, "Random forests," Machine Learning, vol. 45, no. 1, pp. 5–32, 2001. doi.org/10.1023/A:1010933404324

[20] S. Saeb, L. Lonini, A. Jayaraman, D. C. Mohr, and K. P. Kording, "The need to approximate the use-case in clinical machine learning," GigaScience, vol. 6, no. 5, pp. 1–9, 2017. doi.org/10.1093/gigascience/gix019

[21] F. Pedregosa et al., "Scikit-learn: Machine learning in Python," Journal of Machine Learning Research, vol. 12, pp. 2825–2830, 2011. jmlr.org/papers/v12/pedregosa11a.html

[22] P. M. Bossuyt et al., "STARD 2015: An updated list of essential items for reporting diagnostic accuracy studies," BMJ, vol. 351, Art. no. h5527, 2015. doi.org/10.1136/bmj.h5527

How to Cite: Sadyrova Nurgul, Muratov Zhanibek, Tashpolotova Anarkan. (2026). Interpretable lung-field texture analysis of chest radiographs for tuberculosis triage: Segmentation, zonal patterns and the WHO target product profile. Journal of Prevention, Diagnosis and Management of Human Diseases (JPDMHD), 6(2), 54-62. https://doi.org/10.55529/jpdmhd.62.54.62

BIOGRAPHIES OF AUTHORS

	**Sadyrova Nurgul**, holds the post of associate professor in the Department of Clinical Disciplines at Jalal-Abad International University, located in Manas, Kyrgyzstan. As corresponding author of this article, Sadyrova Nurgul is the contact for its evaluation of interpretable lung-field texture analysis of chest radiographs for tuberculosis triage, measured against the World Health Organization target product profile. Email: sadyrova.n73@mail.ru
	**Muratov Zhanibek**, is a full professor whose principal appointment lies in the Department of Clinical Disciplines, Jalal-Abad International University, Kyrgyzstan. Further affiliations link Muratov Zhanibek with Osh State University and Osh International Medical University. The present paper, on segmentation quality and zonal patterns in automated tuberculosis screening from chest X-rays, lists Muratov Zhanibek as second author.
	**Tashpolotova Anarkan**, teaches at lecturer grade within the Department of Clinical Disciplines of Jalal-Abad International University in Manas. Tashpolotova Anarkan joined the author team of this study, which examined how U-Net lung masks, upper-zone texture features and patient age shape the accuracy of computer-aided tuberculosis detection on the Montgomery County radiographs.